



Citation for published version:

Shaw, GA, Stirling, J, Kramar, JA, Moses, A, Abbott, P, Steiner, R, Koffman, A, Pratt, JR & Kubarych, ZJ 2016, 'Milligram mass metrology using an electrostatic force balance', *Metrologia*, vol. 53, no. 5, pp. A86-A94.
<https://doi.org/10.1088/0026-1394/53/5/A86>

DOI:

[10.1088/0026-1394/53/5/A86](https://doi.org/10.1088/0026-1394/53/5/A86)

Publication date:

2016

Document Version

Publisher's PDF, also known as Version of record

[Link to publication](#)

Publisher Rights

Other

Work is copyrighted by the US government and is therefore in the public domain.

University of Bath

Alternative formats

If you require this document in an alternative format, please contact:
openaccess@bath.ac.uk

General rights

Copyright and moral rights for the publications made accessible in the public portal are retained by the authors and/or other copyright owners and it is a condition of accessing publications that users recognise and abide by the legal requirements associated with these rights.

Take down policy

If you believe that this document breaches copyright please contact us providing details, and we will remove access to the work immediately and investigate your claim.



PAPER

Milligram mass metrology using an electrostatic force balance

To cite this article: Gordon A Shaw *et al* 2016 *Metrologia* **53** A86

View the [article online](#) for updates and enhancements.

Related content

- [Realising traceable electrostatic forces despite non-linear balance motion](#)
Julian Stirling and Gordon A Shaw
- [Current state of the art in small mass and force metrology within the International System of Units](#)
Gordon A Shaw
- [History and progress on accurate measurements of the Planck constant](#)
Richard Steiner

Recent citations

- [The Revision of the SI – Towards an International System of Units Based on Defining Constants](#)
M. Stock
- [Current state of the art in small mass and force metrology within the International System of Units](#)
Gordon A Shaw
- [Onsite multikilowatt laser power meter calibration using radiation pressure](#)
Paul A. Williams *et al*

Milligram mass metrology using an electrostatic force balance

Gordon A Shaw¹, Julian Stirling¹, John A Kramar², Alexander Moses¹, Patrick Abbott¹, Richard Steiner¹, Andrew Koffman¹, Jon R Pratt¹ and Zeina J Kubarych¹

¹ Quantum Measurement Division, US National Institute of Standards and Technology (NIST), Gaithersburg, MD, USA

² Engineering Physics Division, US National Institute of Standards and Technology (NIST), Gaithersburg, MD, USA

E-mail: gshaw@nist.gov

Received 31 March 2016, revised 9 June 2016

Accepted for publication 14 June 2016

Published 28 September 2016



Abstract

Although mass is typically defined within the International System of Units (SI) at the kilogram level, the pending SI redefinition provides an opportunity to realize mass at any scale using electrical metrology. We propose the use of an electromechanical balance to realize mass at the milligram level using SI electrical units. An integrated concentric-cylinder vacuum gap capacitor allows us to leverage the highly precise references available for capacitance, voltage and length to generate an electrostatic reference force. Weighing experiments performed on 1 mg and 20 mg artifacts show the same or lower uncertainty than similar experiments performed by subdividing the kilogram. The measurement is currently limited by the stability of the materials that compose the mass artifacts and the changes in adsorbed layers on the artifact surfaces as they are transferred from vacuum to air.

Keywords: mass, force, electrostatic force balance (EFB), milligram, capacitance, voltage, International System of Units

 Online supplementary data available from stacks.iop.org/MET/53/A86/mmedia

(Some figures may appear in colour only in the online journal)

1. Introduction

The measurement of mass is ubiquitous in the modern world. From the smallest subatomic particles, to the largest galactic clusters, determining the value of mass helps to explain how physical systems behave. More pragmatically, measurements of mass help determine the economic value of goods around the world. It is therefore critical to ensure mass is uniformly quantified. Historically, this has meant defining mass with the International Prototype Kilogram (IPK). Sometime in 2018, the kilogram's definition will change. Moving forward it will be linked to a fundamental constant using silicon spheres and the x-ray crystal-density (XRCD) method [1] or using a watt balance to compare the weight of a physical mass to an electromagnetic force via Planck's constant [2]. Watt balances are designed to realize mass at the kilogram level, but similar principles apply to smaller masses as well.

Currently, obtaining a standard with a mass less than a kilogram requires submultiples of the primary standard [3]. Each time a mass is subdivided, relative uncertainty accrues progressively. This uncertainty arises during a measurement from a variety of sources, everything from random thermal fluctuations in the balance to the fluctuation of local gravity for some of the more precise mass measurements. At the level of 1 kg, the relative standard uncertainty in mass is 2×10^{-8} . By the time mass is subdivided to the milligram level, relative uncertainty is approximately 2500 times as large, as shown in figure 1. Extrapolating further, the problem potentially becomes worse; by the time the subdivision process reaches 1 ng, the uncertainty could be as large as the measured mass.

The question arises then whether there is a way around this limitation. Can mass standards be improved from the bottom up? Plenty of things are measured in milligrams and micrograms: pharmaceuticals, nutrients in food, precious metals and

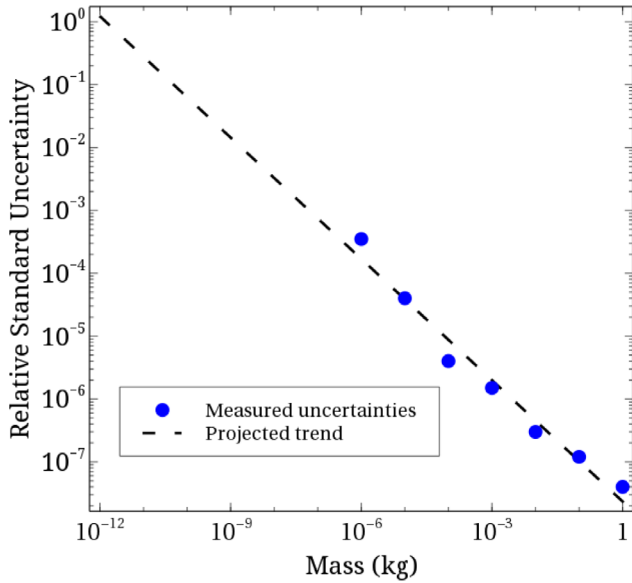


Figure 1. Relative uncertainty in mass as a function of mass value. Dashed line is a linear fit to the data shown.

gems, for example. Most of the current effort has centered on using the Watt balance to define an electronic Kilogram. There are no fundamental limitations that prevent the same principles from scaling to smaller mass measurements. This work describes an approach that also uses electrical measurements to provide a value for mass, but at a smaller scale: an electronic milligram.

2. Theory and traceability

Application of a voltage between conductive elements of a capacitor generates electrostatic force. Several different capacitor geometries have been used to produce electrostatic forces in a balance [4–7]; the NIST (National Institute of Standards and Technology) electrostatic force balance (EFB) uses a concentric cylinder capacitor to generate the force necessary to remain at a null position. The inner cylinder is attached to a movable precision balance mechanism, and the outer cylinder is rigidly attached a fixed laboratory reference frame, as shown in figure 2. The fundamental measurement equation used to realize force between two capacitor elements is

$$F = \kappa V^2, \tag{1}$$

where $\kappa = (dC/dz)/2$, one half the spatial gradient of capacitance between two capacitor elements, C , with respect to their relative displacement, z . F is the resulting electrostatic force from an electric potential V , and is parallel to the direction of the capacitance gradient. In practice, voltage measurements will show an additional surface potential, V_s , originating from patch effect or contact potential difference [8–11], as well as the adsorption of adventitious contaminants onto the capacitor electrodes [12–14]. To account for the surface potential, a voltmeter is used to determine the potential applied between the EFB cylinders to maintain a null position while the applied voltage polarity is reversed. When holding the unloaded balance at null position with a positive or negative voltage, respectively, the measured voltage is given by

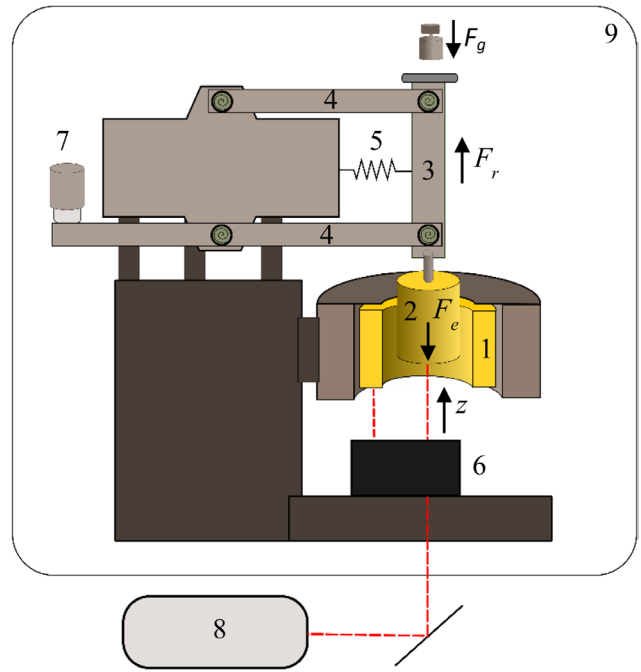


Figure 2. Schematic of the NIST electrostatic force balance (EFB). F_g is gravitational force from a test mass, F_e is electrostatic force from the capacitor, and F_r is the elastic restoring force of the balance mechanism. Components are: outer main capacitor cylinder (1) surrounded by a grounded shield electrode to minimize stray electrical fields, inner main capacitor cylinder (2) (note this cylinder is not electrically connected to the balance mechanism), floating link of 4-bar linkage (3), moving links of 4-bar linkage (4), buckling spring (5), laser interferometer (6), auxiliary capacitor to actuate balance during capacitance gradient measurements (7), interferometer laser (8), vacuum enclosure indicated by solid line (9).

$$V_{Um+} = V_U + V_S, \tag{2}$$

$$V_{Um-} = -V_U + V_S, \tag{3}$$

where V_U is the true potential difference between the capacitor elements in the unloaded state. The force calculated from these two measured potentials is

$$F_{U+} = \kappa V_{Um+}^2 = \kappa(V_U + V_S)^2 = \kappa(V_U^2 + 2V_U V_S + V_S^2), \tag{4}$$

$$F_{U-} = \kappa V_{Um-}^2 = \kappa(V_U - V_S)^2 = \kappa(V_U^2 - 2V_U V_S + V_S^2). \tag{5}$$

The mean of the measured force from the unloaded balance at positive and negative polarity yields

$$F_{Ua} = \kappa(V_U^2 + V_S^2). \tag{6}$$

An analogous expression can be obtained for the balance's loaded state.

$$F_{La} = \kappa(V_L^2 + V_S^2). \tag{7}$$

where the force to balance when loaded with a test mass, results from a potential V_L . Mass is calculated from the difference in force between the loaded and unloaded balances using the polarity reversal process described above as

$$m = \frac{\kappa}{g}(V_L^2 - V_U^2), \tag{8}$$

where g is gravitational acceleration. The V_S^2 terms cancel if the surface potential is constant during the measurement.

Mass realized with the EFB is based on h in a fashion similar to the Watt balance. In the new SI, capacitance will be based on the theoretical equivalence of the von Klitzing constant to e^2/h , realized through quantum Hall resistance, R_H , using an AC/DC resistance to capacitance transfer such that

$$C = \frac{1}{|i\omega R_H|} = \frac{k_c e^2}{2\pi h \Delta\nu(^{133}\text{Cs})_{\text{hfs}}}, \quad (9)$$

where e is the elementary charge, $\Delta\nu(^{133}\text{Cs})_{\text{hfs}}$ is the hyper-fine splitting frequency shift of caesium-133 and k_c is a scaling factor between the quantum hall resistance and measurement of capacitance [15–17]. We note that if capacitance is realized from a calculable capacitor then the measured value of the fine structure constant, α , must be included in k_c . The relative uncertainty of α (3.2×10^{-10}) is too small to have any practical impact on mass realization at current levels of uncertainty.

The displacement of the EFB is measured with an interferometer using a stabilized helium–neon laser. EFB length measurements are related to the vacuum velocity of light, c , by

$$z = \frac{k_z c}{\Delta\nu(^{133}\text{Cs})_{\text{hfs}}}, \quad (10)$$

where k_z is a scaling factor for displacement measurement. Subsequently,

$$\kappa = \frac{k_c}{k_z} \frac{e^2}{4\pi h c}. \quad (11)$$

Measured voltages are traceable to a Josephson junction array, such that

$$(V_L^2 - V_U^2) = (nhk_L \nu_{AC}/2e)^2 - (nhk_U \nu_{AC}/2e)^2, \quad (12)$$

where n is an integer constant denoting the number of junctions used in realization, ν_{AC} is the AC microwave frequency used in the Josephson junction, and k_L and k_U are the voltage ratios of the calibrations necessary to propagate from the Josephson standard to the voltages applied in EFB measurements. Hence,

$$(V_L^2 - V_U^2) = \frac{k_{AC}^2 n^2 h^2 \Delta\nu(^{133}\text{Cs})_{\text{hfs}}^2}{4e^2} (k_L^2 - k_U^2), \quad (13)$$

where k_{AC} is the scaling factor between ν_{AC} and $\Delta\nu(^{133}\text{Cs})_{\text{hfs}}$. An absolute gravimeter in the EFB lab determined gravitational acceleration via length and time measurements (l_g and t_g), so

$$g = \frac{l_g}{t_g^2} = \frac{ck_l \Delta\nu(^{133}\text{Cs})_{\text{hfs}}}{k_t^2}, \quad (14)$$

where k_l is the scaling factor between the measured length and $c/\Delta\nu(^{133}\text{Cs})_{\text{hfs}}$, likewise k_t is the scaling factor between the measured time and $1/\Delta\nu(^{133}\text{Cs})_{\text{hfs}}$. From equation (8), the EFB mass measurements can then be written in terms of the fundamental constants as

$$m = \frac{h \Delta\nu(^{133}\text{Cs})_{\text{hfs}} \Gamma}{c^2}, \quad (15)$$

with scaling factors and other numerical constants collected into

$$\Gamma = \frac{n^2 k_c k_{AC}^2 k_t^2 (k_L^2 - k_U^2)}{16\pi k_l k_z}. \quad (16)$$

Equation (15) links EFB mass directly to Planck’s constant in the same fashion as the Watt balance. Mass realized with an EFB operating according to the principles described above is therefore compatible with the impending SI redefinition of the kilogram.

3. Experimental

3.1. Apparatus

The NIST electrostatic force balance (EFB) [18, 19] was used for all weighings. The EFB is an electromechanical balance mechanism, and is illustrated schematically in figure 2. All measurements are performed in the NIST advanced measurement laboratory in an underground lab at a temperature of 293.15(2) K. Two modes of operation are required. In the capacitance gradient mode, the main capacitor’s inner cylinder translates axially with respect to the outer cylinder to determine the gradient of capacitance with position relative to null position, dC/dz . In the weighing mode, the electrostatic force generated by a concentric cylinder capacitor varies to hold the null position, responding to an external gravitational force in the form of a mass artifact.

The balance mechanism consists of a parallelogram 4-bar linkage where the floating link is mechanically attached to the inner cylinder of the main electrode. This constrains the inner cylinder’s axis to be parallel to the gravitational acceleration vector within the bounds of the parallelism of the ground links. Flexures and an adjustable kinematic mount built into the EFB frame allow parallelism adjustment as described further in the alignments section below. In the capacitance gradient mode, overlap between the two cylinders is controlled with a feedback loop by adjusting the potential applied to an auxiliary electrode on the opposite end of the balance. A 24-bit digital-to-analog converter provides an output voltage to a Kepco BOP 1000 high voltage amplifier⁴, applying up to $\pm 1000\text{V}$ to the auxiliary electrode for position control. A measurement samples 11 equidistant points within 2mm of the travel range of the mechanism. At each point, an Andeen-Hagerling 2500A capacitance bridge measures capacitance. Separate shielded electrical connections are made to the inner and outer cylinders to isolate them from the grounded balance mechanism and vacuum chamber. This ensures the 3-terminal

³ NIST Disclaimer: this article is authored by employees of the U.S. federal government, and is not subject to copyright. Commercial equipment and materials are identified in order to adequately specify certain procedures. In no case does such identification imply recommendation or endorsement by the National Institute of Standards and Technology, nor does it imply that the materials or equipment identified are necessarily the best available for the purpose.

capacitance measurements are insensitive to capacitances other than that measured between the EFB cylinders. A check for stray capacitance is described further below and in the supplement.

A Zygo laser interferometer system provides metrological displacement. This heterodyne interferometer design uses a dual column reference Michelson configuration to measure differential displacement between the bottom of the outer capacitor cylinder and the top of the inner cylinder's inside surface. During capacitance gradient measurements, discrete positions corresponding to the spacing between an integral number of interference fringes were used to avoid polarization mixing errors. Due to the arcuate motion of the balance mechanism's floating link, the capacitance gradient requires a 5th order polynomial fit [20]. Although operating close to the null position renders the higher order terms of the polynomial negligible during weighing experiments, their influence on determinations of the first order term must be quantified to reduce the relative magnitude of this systematic effect to 10^{-6} .

After measuring dC/dz , a relay system switches the high voltage from the auxiliary to the main electrodes. The feedback controller now outputs the voltage necessary to maintain a null position as test masses are placed on and removed from a mass holder attached to the balance's floating link while two Keysight 3458A digital multimeters measure applied voltage. A two-axis mass loading system was used so that the notched mass holder always returns to the same home position during measurement to minimize the effect of the stray force between the movable mass holder and the balance [21, 22]. Two differential weighings with opposite polarity counteract the effect of contact potential as described above. The offset potential is several tens of mV in magnitude.

An adjustable buckling spring attached between the floating link of the 4-bar mechanism and the balance frame reduces the balance stiffness [23]. By moving the balance through part of its range of motion while measuring applied electrostatic force, the balance stiffness can be measured and then minimized to approximately 10^{-3} N m^{-1} by adjusting the buckling spring. Vertical adjustment at the base of the tension spring also allows choice of the operating voltage range. Since applied force is proportional to the square of voltage, the balance can operate at a voltage appropriate for the desired measurement (i.e. the lowest practical voltage), allowing an increase in the sensitivity of the balance for smaller test masses. At equilibrium, the average position within a 0.1 Hz bandwidth is held within approximately 1 nm from the null position. In combination with the balance stiffness, this results in force resolution on the order of piconewtons.

3.2. Alignments

Alignments of the balance mechanism and their contributions to measurement uncertainty are described more fully in supplementary materials (stacks.iop.org/MET/53/A86/mmedia), and are similar to previous work [18]. The uncertainties associated with alignment of the capacitor cylinders, corner

Table 1. Uncertainty components in the EFB mass measurements.

Uncertainty components	Relative magnitude ($k = 1$)	
Type B uncertainties		
Transfer of length ($\delta L/L$)	1×10^{-7}	1×10^{-7}
Transfer of voltage ($2\delta V/V$)	4.0×10^{-6}	4.0×10^{-6}
Transfer of capacitance ($\delta C/C$)	1.2×10^{-7}	1.2×10^{-7}
Alignment of capacitor cylinders	1.2×10^{-7}	1.2×10^{-7}
Corner loading	6.0×10^{-7}	6×10^{-7}
Stray capacitance	8.2×10^{-7}	8.2×10^{-7}
Hysteresis	1.4×10^{-6}	2.2×10^{-7}
Alignment of balance travel	7.3×10^{-7}	7.3×10^{-7}
Temperature dependence of dC/dz	4.4×10^{-6}	4.4×10^{-6}
Type A uncertainties		
Weighing	3.8×10^{-6}	2.2×10^{-6}
Combined standard uncertainty	7.3×10^{-6}	6.5×10^{-6}

loading, and alignment of the balance travel to gravity appear in table 1. These procedures align the electrostatic force vector to gravity at the null position, since the cylindrical geometry of the capacitor ensures the radial forces cancel and the balance mechanism is very compliant parallel to gravity and very stiff in other directions.

3.3. Electrical calibrations

An Andeen-Hagerling 2500A 1 kHz capacitance bridge was used for all capacitance measurements. The calibration of the capacitance bridge included an internal calibration of the circuitry and transformers as well as an external calibration using a NIST 10 pF reference standard capacitor. The external calibration procedure calibrated the bridge to the stored reference capacitance value at 1 KHz. The calibrated bridge was then used to measure the reference value using the stored calibration state. Agreement was obtained to $0.024 \mu\text{F F}^{-1}$ with an expanded uncertainty ($k = 2$) of $0.246 \mu\text{F F}^{-1}$ at 10 pF. The expanded uncertainty ($k = 2$) of the 10 pF NIST reference standard value at 1 kHz was $0.100 \mu\text{F F}^{-1}$. The bridge was also checked against 100 pF and 1 pF reference standards near the time of the external calibration. The 100 pF bridge agreement with the reference standard was $0.022 \mu\text{F F}^{-1}$ and the 1 pF bridge agreement with the reference value was $0.20 \mu\text{F F}^{-1}$.

Keysight 3458A digital voltmeters (DVMs) were used to determine voltage, and were calibrated against a Fluke 5720 that had been calibrated via 1V and 10V Zener references (calibrated against the NIST Josephson Voltage Standard) and a resistive divider bridge. The linearity of the 5720 on the 1100V range was checked against various ratios on the resistive divider and found to have a linearity within about $0.2 \mu\text{V V}^{-1}$ of full scale (1000V). The non-linearity of the DVMs is corrected for during post processing. Although the relative calibration uncertainty of the voltmeters was less than 1×10^{-6} , differences of 2×10^{-6} were found between the readings of the two voltmeters used in parallel during the EFB measurements. We use this as our estimate of the voltage uncertainty, since tests have confirmed that this difference does not arise from internal DVM temperature fluctuations or cable resistance.

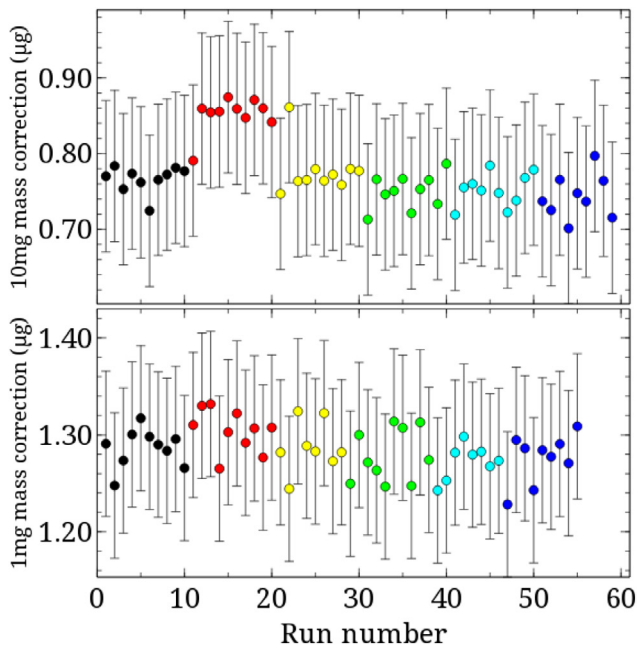


Figure 3. Mass correction values (difference from 1 mg and 10 mg) and uncertainties for 1 mg and 10 mg check standards, respectively, used in subdivision. Different colors indicate trials performed on separate days as part of the workdowns used for the comparison to EFB values, error bars represent combined uncertainty at $k = 1$ [3].

3.4. Mass calibrations by subdivision from the kilogram

A cross-check experiment was carried out to compare the EFB mass values with values determined by kilogram subdivision. Three separate commercial robotic mass comparison systems were used in the subdivision of mass from a kilogram to a milligram. These robots employ high-precision mass comparators that span the ranges 1 kg to 100 g, 100 g to 1 g, and 1 g to 1 mg, respectively. Each system consists of a mass comparator, a three axis robotic arm, a system control unit, and a weight magazine. Compared to traditional manual subdivision measurements, robotic comparators have the potential to achieve more precise mass measurements. The highly repeatable motion of robotic arms results in precise positioning and placement of weights onto the comparator weighing pans, thus decreasing measurement variance. Furthermore, the absence of human interaction in the measurement process prevents temporal heating effects on the weights and weighing cell response. Weighing designs can be programmed to run continuously for hours or days. Environmental data (temperature, pressure, and humidity) is automatically collected and was used to calculate a buoyancy correction, which has been applied to all reported results.

Mass dissemination by subdivision from a kilogram to a milligram requires 6 series of weighing schemes, one per decade. Measurements of each decade are repeated 10 times; the results for each weight are approximately normally distributed, so the means are taken as final mass values. The smallest mass in a given series is used as the restraint for the following decade. This process is repeated for every decade in a mass set. A control chart for 1 mg and 10 mg masses used in the workdown is shown in figure 3.

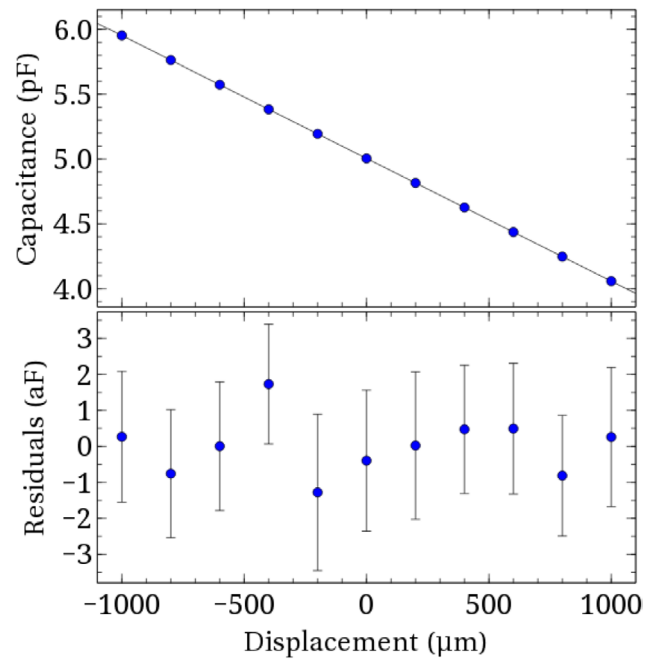


Figure 4. EFB positional capacitance gradient. Fifth order polynomial fit (top) and fit residuals (bottom). Error bars show one standard deviation of measured residuals.

4. Results and data analysis

4.1. Measurement results

Figure 4 shows a 5th order polynomial fit, illustrating a typical dC/dz measurement. Here, a separate polynomial is fit to the average capacitance of each position sweep as a function of time, and then the fit is subtracted from the data to compensate for position drift. The value of the capacitance gradient for a particular measurement is calculated as the mean of the gradients over the course of that measurement. The capacitance gradient measurements bracket the weighings at a regular interval so that the average of the capacitance gradient before and after a particular weighing is used to determine the value of mass for that experimental trial.

Figure 5 shows the force calculated using equation (1) from a 1 mg nominal aluminum wire mass artifact. V here is the voltage measured using the DVM. F_{U+} , F_{U-} , F_{L+} and F_{L-} , correspond to electrostatic force measured in the unloaded state at positive and negative polarity, and the loaded state at positive and negative polarity, respectively. The balance restoring force, and hence the operating voltage, clearly drifts during the measurements. A temporal function $F_{U+}(t)$ is derived from linear interpolation between consecutive determinations of F_{U+} with measured timestamp, t . The mass, m_p , in a particular weighing trial is

$$m_p = [F_{U-,p} - F_{U+}(t_{U-,p}) - F_{L+,p} + F_{U+}(t_{L+,p}) - F_{L-,p} + F_{U+}(t_{L-,p})]/2g, \tag{17}$$

where p is an index denoting the number of the trial and $t_{U-,p}$, $t_{L+,p}$, and $t_{L-,p}$ are the measured timestamps for $F_{U-,p}$, $F_{L+,p}$, and $F_{L-,p}$, respectively.

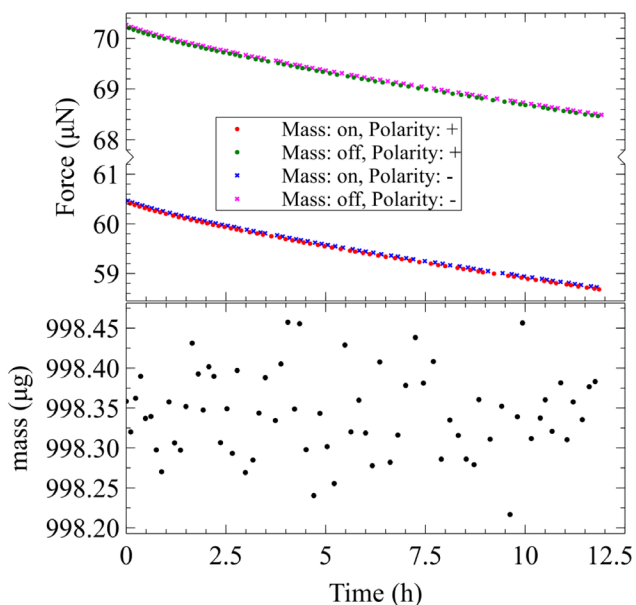


Figure 5. EFB weighing data. Calculated force, F , over time during weighing experiments, top. Notice that the balance force is higher when the mass is off compared to when it is on the balance. This is because the balance is adjusted to rest in an upward position so that the electrostatic force on the capacitor can pull it down. The addition of a mass to the balance reduces the amount of restoring force that must be applied, hence the decrease in F . Note the broken vertical axis. Measured mass, m_p , of a 1 mg artifact, bottom. The hysteresis correction has not yet been applied to these data.

Table 2. EFB values for 2016 weighings.

EFB mass values and combined uncertainties ($k = 1$)	
0.998 3245(73) mg	20.916 92(14) mg

Measurements were also performed on a 20 mg gold wire mass (calibrated also in 2006 [18]). A summary of EFB mass values and combined standard uncertainties are shown in table 2. These values are the mean of the 2016 EFB measurements shown in figure 6.

4.2. Uncertainty analysis

Table 1 summarizes the results of an uncertainty analysis of the EFB mass measurements. Type B uncertainties in voltage, capacitance, alignment and corner loading error are described above and in the supplement. Length uncertainty is taken from the accuracy specification of the measurement electronics to be the least significant bit in the displacement measurement electronics divided by the 2 mm maximum displacements used in the dC/dz determination. The frequency dependence of the capacitance as well as the parasitic capacitance gradient between the outer capacitor cylinder and balance mechanism are both shown to be negligible with an analysis detailed in the supplement.

4.2.1. Balance hysteresis. Balance hysteresis arises from motion in the flexures connecting the members of the 4-bar linkage. A small hysteresis in force may arise from transient motion of the balance mechanism when the test mass first

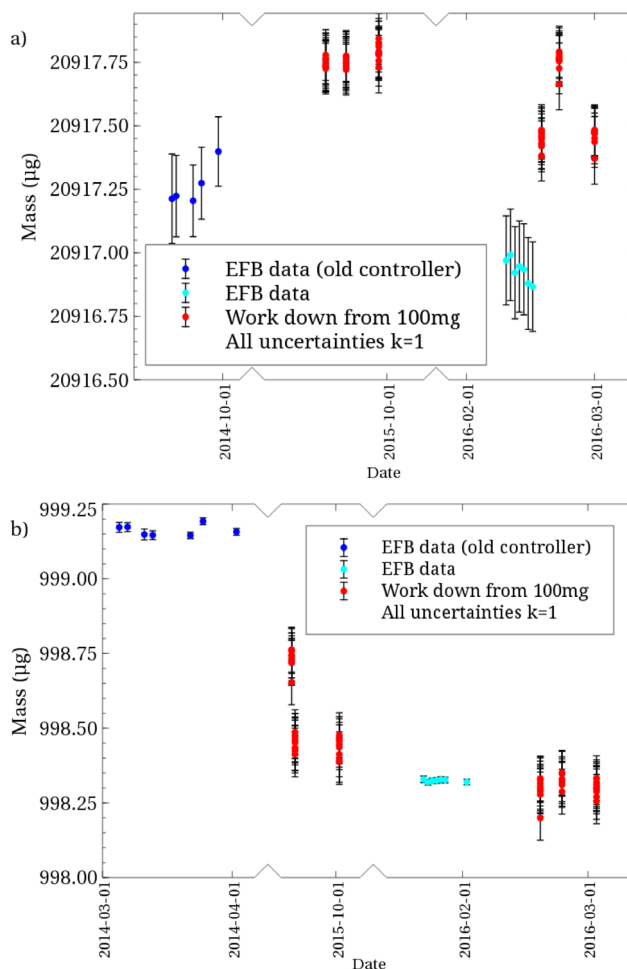


Figure 6. Comparison of gold 20 mg (a) and aluminum 1 mg (b) masses. Error bars on the EFB results are calculated at $k = 1$ using the type B uncertainties from table 1 and type A uncertainty calculated from the standard deviation of the mean for the mass measurements collected during each daily trial.

contacts the balance, or when it is first lifted off. In addition, there is often a small balance excursion as the gain of the position control feedback is reduced prior to measuring applied voltage. This hysteresis force was directly measured by simulating the placement of a mass on the balance with a short position excursion programmed into the position control followed by a gain change at the same approximate operating voltage level used for a particular mass. The short excursions/gain changes mimicked the transients occurring when the masses are deposited onto and then removed from the balance during a weighing. To estimate uncertainty from hysteresis, an identical experiment was conducted to measure hysteresis force with a position excursion 10 times as long in time as that measured for the 1 mg mass measurements. The measured hysteresis force changed by approximately 10%. We therefore use 10% of the measured hysteresis force as our type B uncertainty for hysteresis. The magnitude and uncertainty of the hysteresis correction to the mass values are summarized in table 3.

4.2.2. Temperature dependence of capacitance gradient. A small dependence of the capacitance gradient on the balance temperature may be affecting the measurement.

Table 3. Summary of balance hysteresis and uncertainty.

Mass artifact	1 mg	20 mg
Balance hysteresis	13.9 (1.4) ng	49.7(4.7) ng

Note: These quantities are subtracted from measured mass such as that shown in figure 3 to obtain the final mass values shown in table 2.

Directly after pumping the system to vacuum, a pronounced temperature change occurs. During this time, the balance capacitance gradient and temperature were monitored. A linear fit to the data reveals a shift of approximately 4.2×10^{-15} F m⁻¹ decrease in dC/dz per K. The balance temperature during weighings gradually drifts upward by as much as 10 mK as a result of heat generated by the automated mass exchange system and then back downward during dC/dz measurements. Given the magnitude of dC/dz is approximately 0.947 nF m⁻¹, we add a relative uncertainty of 4.4×10^{-6} to account for this effect, stipulating that data collection will not commence until the average temperature measured during consecutive capacitance gradient determinations is constant at the level of 10 mK.

4.2.3. Statistical uncertainty. The mass measurements were replicated on at least 3 days, with at least 75 measurements of m_p per day and a capacitance gradient measurement bracketing each daily measurement. The statistical (type A) uncertainty quoted in table 1 is the standard deviation of these consecutive daily values. It includes statistical uncertainty in both the weighing process and the capacitance gradient determination. The uncertainty calculated with this method is approximately the same as the standard deviation of the mean calculated within a particular daily measurement, indicating that a single day's weighing will likely be sufficient to describe the statistical uncertainty of the measurement.

5. Discussion

In order to confirm that the EFB mass value is functionally equivalent to subdivision from the kilogram, a comparison of two different masses was carried out. Figure 6 summarizes the results of three cross-check experiments over a time period of over 2 years. Another measurement of the 20mg mass was published ten years earlier [18], and resulted in an EFB value of 20.91769(45) mg, as compared to a subdivision value of 20.91905(35) mg where parentheses denote combined standard uncertainty. Between each EFB measurement, the balance mechanism was disassembled, modified and realigned. Three different control systems were used over the course of the work. The first control system operated in the first part of the 2005 measurements, the second operated in the second part of the 2005 measurements and the 2014 measurements, the third operated in the 2016 measurements. Three different analysis methods were also used. Important differences between the 2005, 2014 and 2016 measurements include the change from a linear fitting algorithm used for the 2005 capacitance gradient to a cubic polynomial fit used for the 1 mg results from 2014, and finally a fifth-order fit [20] for the 20 mg results from 2014, and all results in 2016. The 2014 and 2016 measurements also used the interleaved

capacitance gradient determinations, whereas the 2005 measurement was the average of all the capacitance gradients determined over the course of several months. The most recent control system and analysis method are described in this paper, and represent best current practice. Finally, different operators carried out the measurement each time.

At the 1 mg level, it is apparent that the mass itself changed substantially over time, losing almost 1 microgram over the course of two years, with one abrupt change evident during a subdivision calibration. When measurements are performed in close temporal proximity, the relative difference between the EFB and subdivision values is 1.5×10^{-5} . This indicates agreement of the two results at $k = 1$.

At the 20 mg level, there was also a slight decrease in the mass over time, however the more recent measurements show there is a significant difference between the EFB and subdivision methods. The EFB mass value is between 0.4 μg and 1 μg lower. Although the difference between the measured values is substantially smaller than in previous work [18], the measurement uncertainties are smaller as well. 1 mg and 10 mg check standards used in the subdivision measurements did not show the same level of instability as the gold wire mass, as shown in figure 3. It is important to note that the relative discrepancy between the two values is at most 5×10^{-5} , within the acceptable range for current primary calibrations in this mass range.

A potential source of systematic differences between the two weighing methods is the surface chemistry of the mass artifacts. The surface of the gold wire used for the 20 mg artifact may have a substantial water layer. Scanning probe microscope (SPM) studies report water layer thicknesses as large as 30 nm under ambient laboratory conditions similar to ours [24]. This would result in a mass contribution of approximately 0.5 μg (assuming the bulk density of water, and using the dimensions of the mass). Desorption of the water layer may therefore account for the differences between the mass measurements performed in vacuum using the EFB and in air using the robotic mass comparator.

The aluminum wire used for the 1 mg artifact likely forms an oxide layer primarily composed of amphoteric aluminum hydroxide [25, 26] in a partially hydrated pseudo-bohemite structure. Residual gas analysis studies show that water is the dominant component in vacuum outgassing of Al surfaces stored under laboratory conditions [27, 28]. The water appears to predominantly come from the partial dehydration of the pseudo-bohemite, AlO(OH), to Al₂O₃ in a 2:1 stoichiometric ratio [26]. Extensive surface water layers only form on aluminum oxide surfaces at relative humidity above 70% [29, 30], much higher than the 40% maintained in our laboratories. Using the approximate oxide thickness of 3.5 nm determined with x-ray photoelectron spectroscopy (XPS) [26], the density of bohemite (3×10^3 kg m⁻³) [31] and dimensions of the Al wire mass (5 cm long, and 100 μm in diameter), the total oxide mass would be approximately 0.2 μg for the 1 mg mass used. The total change in oxygen concentration in the film after introduction into vacuum and heating to 300 °C is 2.3% [26]. Since oxygen makes up 29% of the bohemite mass, a conservative estimate of the total mass change from aluminum surface dehydration would be 1 ng. Although it is outside the scope of the current work, further study may

be required to clarify the role of surface chemistry in air to vacuum mass transfer and choose a suitable material and fabrication method for mass artifacts used in vacuum to air comparisons performed at the milligram level. Previous work to determine appropriate corrections for adsorbed layers on mass artifacts has been summarized elsewhere [32], and methods currently under development will allow direct comparison between masses in air and vacuum [33].

Finally, a 50 μg artifact was weighed. Although a detailed examination of the micromass results are beyond the scope of the current work, significant reductions in uncertainty are apparent using electrostatics relative to those expected from subdivision. Extrapolation of the trend in mass uncertainty in figure 1 indicates a relative standard uncertainty of approximately 10^{-3} can be expected at 50 μg , and this result is approximately consistent with current published micromass uncertainties [34–36]. The EFB mass value is 50.633(14) μg , so the uncertainty of this preliminary result is about an order of magnitude lower than current methods. A detailed examination of micromass calibration is left for future work, but the first of these measurements indicates that the EFB should provide an improvement in scaling of SI mass metrology for even smaller masses.

6. Conclusion

Milligram-level masses can be accurately and traceably calibrated via the fundamental constants using an electrostatic force balance (EFB) with uncertainty suitable for commerce and national metrology institutes. Results of comparisons between electrostatic mass metrology and subdivision from the kilogram agree within less than a relative difference of 5×10^{-5} over more than 10 years despite multiple instrumentation, operator and methodology changes in both methods. Recent advances allow relative uncertainties in the parts-per-million range at $k = 1$ in vacuum, as demonstrated in an uncertainty analysis for the EFB. Small mass metrology is now primarily limited by systematic uncertainty, likely dominated by the surfaces of the mass artifacts themselves as they change physically from abrasion or accretion of particulates or due to desorption of surface layers in transfer between air and vacuum.

Acknowledgments

The authors gratefully acknowledge David Newell and Neil Zimmerman of the NIST Quantum Measurement Division for helpful discussions on SI metrology and frequency dependence of capacitance measurements, respectively.

References

- [1] Mana G et al 2015 The correlation of the N_A measurements by counting ^{28}Si atoms *J. Phys. Chem. Ref. Data* **44** 031209
- [2] Schlamminger S, Haddad D, Seifert F, Chao L S, Newell D B, Liu R, Steiner R L and Pratt J R 2014 Determination of the Planck constant using a watt balance with a superconducting magnet system at the National Institute of Standards and Technology *Metrologia* **51** S15
- [3] Jabbour Z and Yaniv S 2001 The kilogram and measurements of mass and force *J. Res. Natl. Inst. Stand. Technol.* **106** 25–46
- [4] Sienknecht V and Funck T 1986 Realization of the SI unit volt by means of a voltage balance *Metrologia* **22** 209
- [5] Bego V, Butorac J and Ilic D 1999 Realization of the kilogram by measuring at 100 kV with the voltage balance ETF *IEEE Trans. Instrum. Meas.* **48** 212–5
- [6] Nesterov V, Mueller M, Frumin L L and Brand U 2009 A new facility to realize a nanonewton force standard based on electrostatic methods *Metrologia* **46** 277–82
- [7] Chen S-J and Pan S-S 2011 A force measurement system based on an electrostatic sensing and actuating technique for calibrating force in a micronewton range with a resolution of nanonewton scale *Meas. Sci. Technol.* **22** 045104
- [8] Kelvin L 1898 V. Contact electricity of metals *Phil. Mag. Ser. 5* **46** 82–120
- [9] Smoluchowski R 1941 Anisotropy of the electronic work function of metals *Phys. Rev.* **60** 661–74
- [10] Bouwman R and Sachtler W M H 1970 Photoelectric determination of the work function of gold–platinum alloys *J. Catal.* **19** 127–39
- [11] Nonnenmacher M, O’Boyle M P and Wickramasinghe H K 1991 Kelvin probe force microscopy *Appl. Phys. Lett.* **58** 2921–3
- [12] Nieuwenhuys B E, Bouwman R and Sachtler W M H 1974 The changes in work function of group Ib and VIII metals on xenon adsorption, determined by field electron and photoelectron emission *Thin Solid Films* **21** 51–8
- [13] Rossi F and Opat G I 1992 Observations of the effects of adsorbates on patch potentials *J. Phys. Appl. Phys.* **25** 1349–53
- [14] Darling T W, Rossi F, Opat G I and Moorhead G F 1992 The fall of charged particles under gravity: a study of experimental problems *Rev. Mod. Phys.* **64** 237–57
- [15] Jeffery A, Elmquist R E, Shields J Q, Lee L H, Cage M E, Shields S H and Dziuba R F 1998 Determination of the von Klitzing constant and the fine-structure constant through a comparison of the quantized Hall resistance and the ohm derived from the NIST calculable capacitor *Metrologia* **35** 83–96
- [16] Schurr J, Ahlers F and Kibble B P 2012 The ac quantum Hall resistance as an electrical impedance standard and its role in the SI *Meas. Sci. Technol.* **23** 124009
- [17] Kalmbach C-C, Schurr J, Ahlers F J, Müller A, Novikov S, Lebedeva N and Satrapinski A 2014 Towards a graphene-based quantum impedance standard *Appl. Phys. Lett.* **105** 073511
- [18] Pratt J R and Kramar J A 2006 SI realization of small forces using an electrostatic force balance *Proc. XVIII IMEKO World Congress on Metrology for a Sustainable Development (Rio de Janeiro, Brazil, 17–22 September 2006)* p 109
- [19] Kim M-S, Pratt J R, Brand U and Jones C W 2012 Report on the first international comparison of small force facilities: a pilot study at the micronewton level *Metrologia* **49** 70–81
- [20] Stirling J and Shaw G A 2016 Realising traceable electrostatic forces despite non-linear balance motion (in preparation)
- [21] Jones C W, Kramar J A, Davidson S, Leach R K and Pratt J R 2008 Comparison of NIST SI force scale to NPL SI mass scale *Proc. ASPE (Portland, OR USA, 19–24 October 2008)* pp 1–4
- [22] Chen S-J, Pan S-S and Lin Y-C 2014 Comparison of milligram scale deadweights to electrostatic forces *Acta Imeko* **3** 68–72
- [23] Pratt J R, Newell D B and Kramar J A 2002 A flexure balance with adjustable restoring torque for nanonewton force measurement *Proc. IMEKO Joint Int. Congress (Celle, GE, 24–26 September 2002)* *VDI-Berichte* **1685** 77–82

- [24] Freund J, Halbritter J and Hörber J K H 1999 How dry are dried samples? Water adsorption measured by STM *Microsc. Res. Tech.* **44** 327–38
- [25] Wefers K and Misra C 1987 Oxides and hydroxides of aluminum 1987 *Aluminum Corporation of America Technical Note*
- [26] Alexander M R, Thompson G E and Beamson G 2000 Characterization of the oxide/hydroxide surface of aluminium using x-ray photoelectron spectroscopy: a procedure for curve fitting the O 1s core level *Surf. Interface Anal.* **29** 468–77
- [27] Dylla H F, Manos D M and LaMarche P H 1993 Correlation of outgassing of stainless steel and aluminum with various surface treatments *J. Vac. Sci. Technol. A* **11** 2623–36
- [28] Edwards D 1977 An upper bound to the outgassing rate of metal surfaces *J. Vac. Sci. Technol.* **14** 1030–2
- [29] Missert N A and Copeland R 2006 Scanning probe studies of water at the aluminum surface *Appl. Surf. Sci.* **1** 219–24
- [30] Missert N and Copeland R G 2008 Scanning probe studies of water nucleation on aluminum oxide and gold surfaces *Appl. Surf. Sci.* **254** 1972–6
- [31] Anon 2015 *CRC Handbook of Chemistry and Physics* (London: Taylor and Francis)
- [32] Gläser M and Borys M 2009 Precision mass measurements *Rep. Prog. Phys.* **72** 126101
- [33] Jabbour Z J, Abbott P, Williams E, Liu R and Lee V 2009 Linking air and vacuum mass measurement by magnetic levitation *Metrologia* **46** 339–44
- [34] Madec T, Mann G, Meury P-A and Rabault T 2007 Micro-mass standards to calibrate the sensitivity of mass comparators *Metrologia* **44** 266–74
- [35] Hu M H, Wang J, Zhang Y, Cai C Q, Zhong R L, Yao H and Ding J A 2012 Research on micro-gram weight standards below 1 mg in NIM *Proc XX IMEKO World Congress, Metrology for Green Growth (Busan, Republic of Korea, 9–14 September 2012)* p 37477
- [36] Ștefănescu D M and Vălcu A 2014 Means for ensuring SI traceability of microforces and/or micromasses *Proc IMEKO XXII (Cape Town, Republic of South Africa, 3–5 February 2014)*